Supplementary material

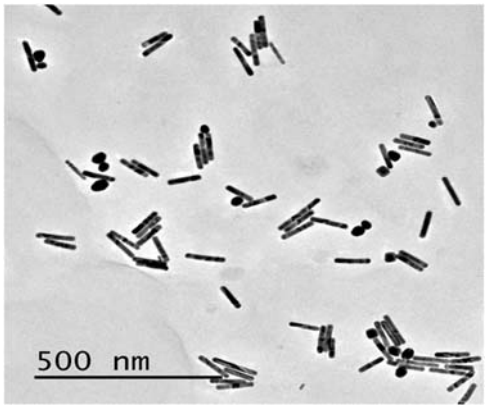

Figure S1: Large scale AuNRs TEM image. (Scale 500 nm).

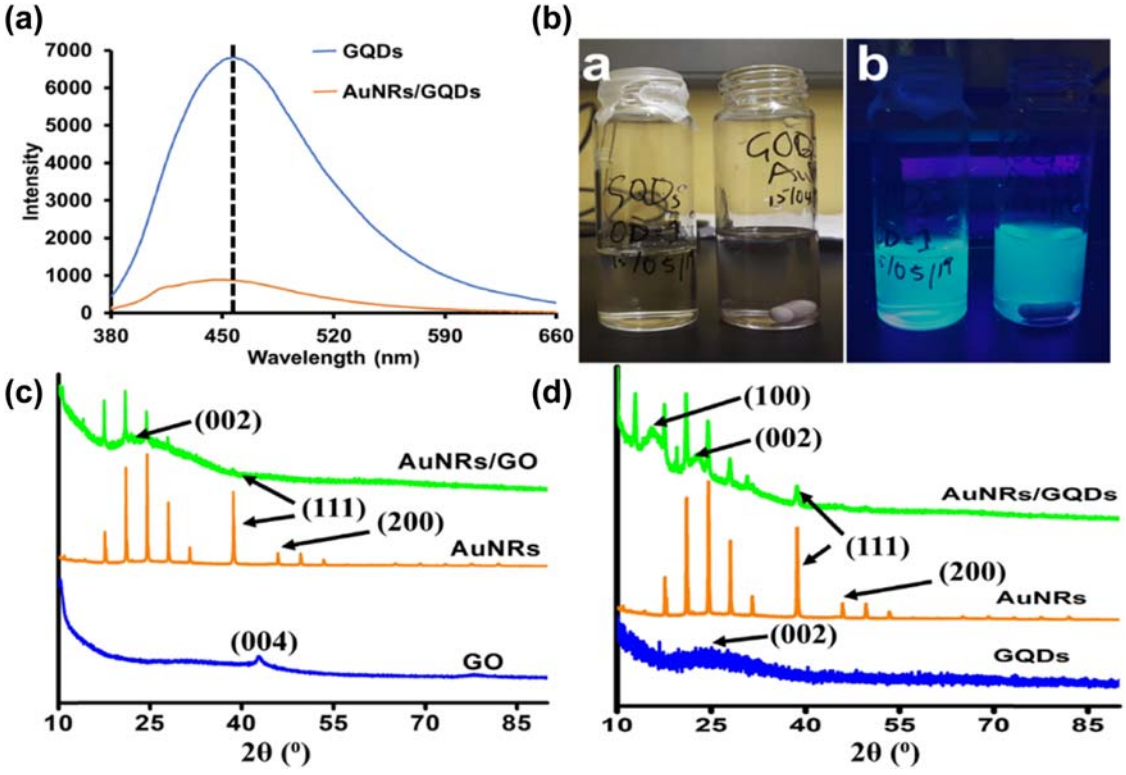

Figure S2: GQDs and AuNRs/GQDs (a) PL spectrum and (b) photographic image in the (a) normal lighting and (b) under UV lights. XRD patterns of (c) AuNRs/GO and (d) AuNRs/GQDs.

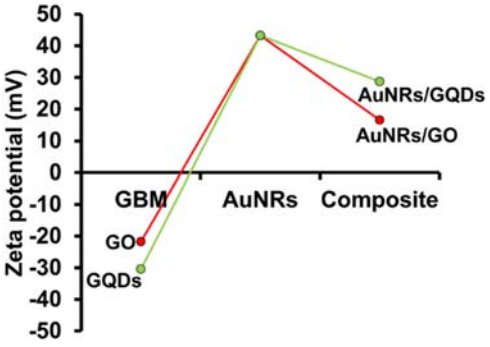

Figure S3: Zeta potential of GO, GQDs, AuNRs, and composites.

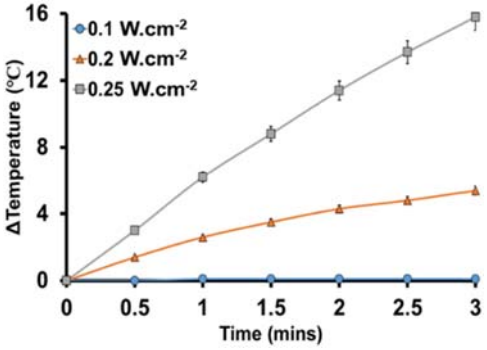

Figure S5: The temperature change of deionized water when irradiated with different laser power densities.

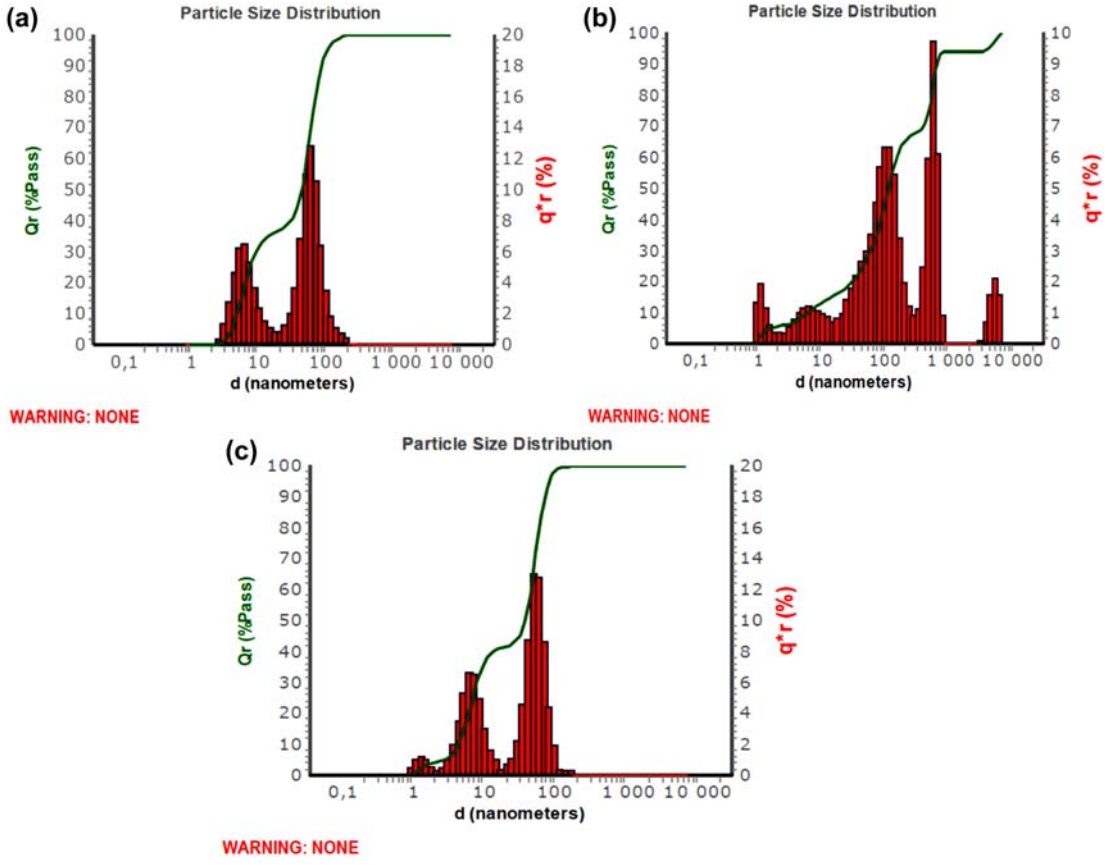

Figure S4: The Hydrodynamic size distribution of (a) AuNRs, (b) AuNRs/GO and (c) AuNRs/GQDs.

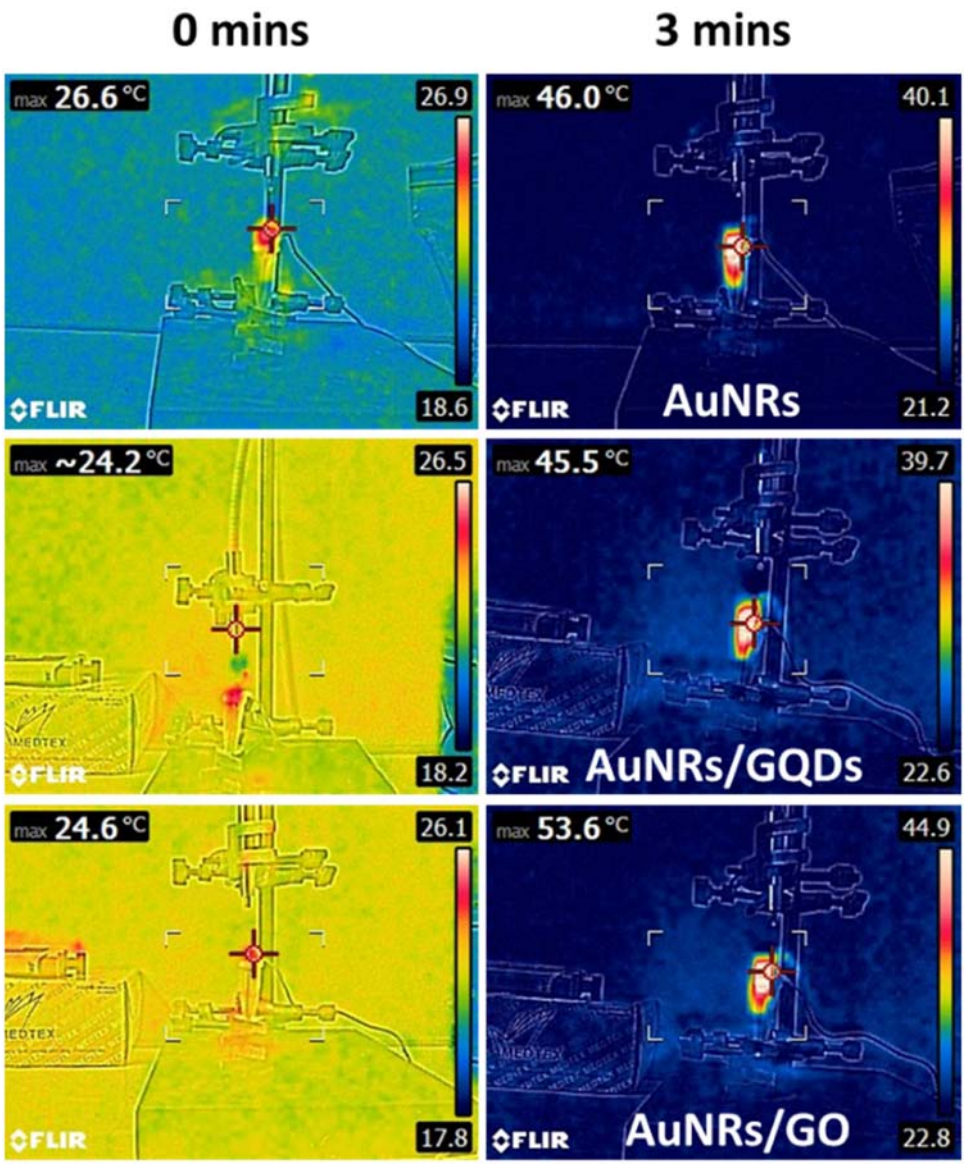

Figure S6: The temperature change from 0 mins and 3 mins of AuNRs, AuNRs/GO and AuNRs/GQDs (50 μg. mL^{-1}) when irradiated with with NIR laser (1064 nm) at 0.2 $W.cm^{-2}$.

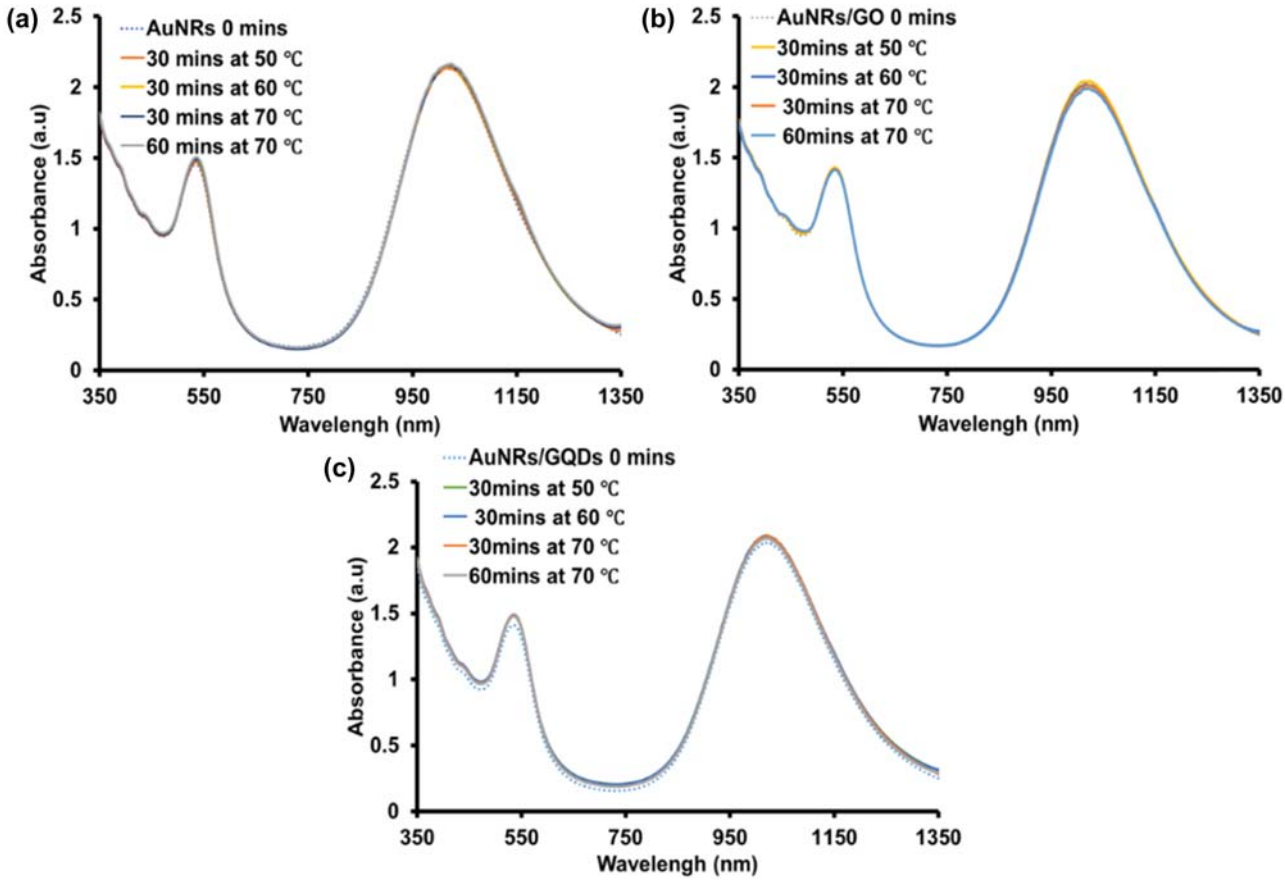

Figure S7: Thermal stability of A) AuNRs B) AuNRs/GO and C) AuNRs/GQDs incubated at 50°C, 60°C, 70°C for 30°C mins and 60°C mins at 70°C.

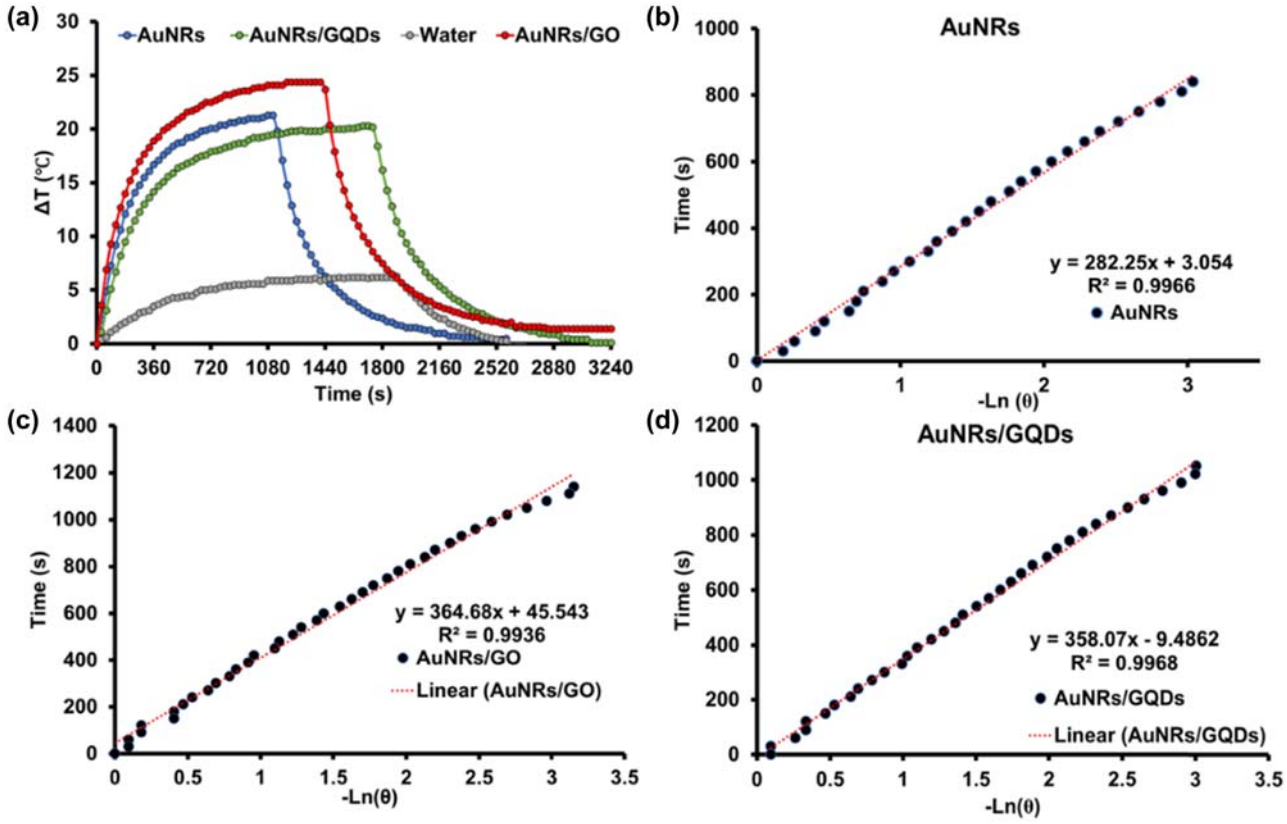

Figure S8: (a) Temperature changes with time upon laser irradiation and the cooling process when the laser is off (1064 nm laser, 0.2 W.cm^{-2}) for denoised water, AuNRs, AuNRs/GO and AuNRs/GQDs. (b) AuNRs linear-time data versus -ln(θ) obtained from the cooling period. (c) AuNRs/GO linear-time data versus -ln(θ) obtained from the cooling period. (d) AuNRs/GQDs linear-time data versus -ln(θ) obtained from the cooling period.